Estuaries and Coasts
https://doi.org/10.1007/s12237-020-00783-4

Effects of Ferrous Iron and Hydrogen Sulfide on Nitrate Reduction in the Sediments of an Estuary Experiencing Hypoxia

Helena Jäntti[1] · Sanni L. Aalto[1,2] · Hans W. Paerl[3]

Received: 19 February 2020 / Revised: 13 May 2020 / Accepted: 10 June 2020

Abstract

Hypoxia is common feature of eutrophic estuaries and semi-enclosed seas globally. One of the key factors driving hypoxia is nitrogen pollution. To gain more insight into the effects of hypoxia on estuarine nitrogen cycling, we measured potential nitrate reduction rates at different salinities and levels of hypoxia in a eutrophic temperate microtidal estuary, the Neuse River Estuary, North Carolina, USA. We also tested the effect of hydrogen sulfide and ferrous iron additions on the nitrate reduction pathways. Overall, DNRA dominated over denitrification in this periodically hypoxic estuary and there was no correlation between the potential nitrate reduction rates, salinity, or dissolved oxygen. However, when hypoxia lasted several months, denitrification capacity was almost completely lost, and nearly all nitrate added to the sediment was reduced via DNRA. Additions of hydrogen sulfide stimulated DNRA over denitrification. Additions of ferrous iron stimulated nitrate consumption; however, the end product of nitrate consumption was not clear. Interestingly, substantial nitrous oxide formation occurred in sediments that had experienced prolonged hypoxia and were amended with nitrate. Given expanding hypoxia predicted with climate change scenarios and the increasing nitrate loads to coastal systems, coastal sediments may lose their capability to mitigate nitrogen pollution due to DNRA dominating over denitrification during extended hypoxic periods.

Keywords Denitrification · DNRA · Nitrous oxide · Estuaries · Hypoxia · Sediment

Introduction

The amount of reactive nitrogen (N) in the environment has increased dramatically during the past 150 years, which has promoted eutrophication of coastal waters (Paerl and Piehler 2008). One of the most severe symptoms of eutrophication is hypoxia (oxygen (O_2) 90 μmol l^{-1} at STP) (Diaz and Rosenberg 1995, 2008; Breitburg et al. 2018), which alters biogeochemical cycling of numerous key elements (e.g., carbon, nitrogen, sulfur, phosphorus).

Microbes in coastal sediments provide an important ecosystem service by converting reactive N through microbial pathways to dinitrogen (N_2) and nitrous oxide (N_2O) gases (Seitzinger 1988; Dalsgaard et al. 2005). It has been estimated that globally, coastal and shelf areas remove approximately of 25% of the total fluvial reactive N input (Sharples et al. 2017). However, under hypoxic conditions, N removal in coastal sediments decreases, since nitrate (NO_3^-) is also reduced to ammonium (NH_4^+), instead of to N_2 and N_2O, via the dissimilatory nitrate reduction to ammonia (DNRA) pathway (An and Gardner 2002; Gardner et al. 2006; Dong et al. 2011). DNRA can be performed by fermentative heterotrophic organisms, which use organic carbon as the electron donor and by chemolithoautotrophic organisms, which use reduced inorganic compounds as an electron donor (Giblin et al. 2010). In general, fermentative processes are slow and

Communicated by Marco Bartoli

Electronic supplementary material The online version of this article (https://doi.org/10.1007/s12237-020-00783-4) contains supplementary material, which is available to authorized users.

✉ Helena Jäntti
helena.jantti@uef.fi

Sanni L. Aalto
sheaa@aqua.dtu.dk

Hans W. Paerl
hpaerl@email.unc.edu

[1] Department of Environmental and Biological Sciences, University of Eastern Finland, Yliopistonranta 1 E, 70211 Kuopio, Finland

[2] Present address: Section for Aquaculture, Technical University of Denmark, Hirtshals, Denmark

[3] Institute of Marine Sciences, University of North Carolina at Chapel Hill, Morehead City, NC, USA

Published online: 04 July 2020

fermentative DNRA cannot compete with dentification for NO_3^- unless the carbon the NO_3^- ratio is very high (Kraft et al. 2014). Chemolithoautotrophic DNRA in the other hand is not dependent on the availability of organic carbon (An and Gardner 2002; Gardner et al. 2006; Dong et al. 2011). Under benthic anoxia, sedimentary nitrification, which typically provides most substrate for the NO_3^- reducing processes (i.e., Hietanen and Kuparinen 2008), ceases and thus DNRA rates are also inhibited due to the low availability of electron acceptors. Hence, hypoxia can lead to a vicious cycle of eutrophication where the excess bioavailable N builds up, preventing recovery from this process (Jäntti and Hietanen 2012).

Sulfate (SO_4^{2-}) is highly available in marine ecosystems (Canfield 1989 and references therein) and a common consequence of hypoxia is the accumulation of toxic hydrogen sulfide (H_2S) in the bottom water. H_2S is produced when, in the absence of O_2, organic matter is oxidized with SO_4^{2-} (Middelburg and Levin 2009). H_2S affects sedimentary N cycling by inhibiting nitrification and anammox (Joye and Hollibaugh 1995; Hannig et al. 2007), while stimulating chemolithotrophic denitrification and DNRA (Brettar and Rheinheimer 1991; An and Gardner 2002; Gardner et al. 2006; Dong et al. 2011). Hence, hypoxia creates favorable conditions for DNRA; however, the presence of this process is still poorly quantified in estuarine systems.

H_2S is often bound to iron (Fe) compounds, which can also be abundant in estuaries and coastal areas. The interactions between H_2S, Fe, and various forms of N are currently poorly understood. The reactions between NO_3^-, nitrite (NO_2^-), and reduced Fe, which regulate the bioavailability of N, were initially considered to be mainly abiotic (Moraghan and Buresh 1977; Buresh and Moraghan 1976). However, Straub et al. (1996) showed that Fe oxidation with NO_3^- can also be microbially mediated and since then the number of microbial taxa known to be capable for anaerobic Fe^{2+} oxidation with NO_3^- under dark circumneutral conditions has increased substantially (Weber et al. 2006). The magnitude of microbial Fe oxidation with NO_3^- has, however, been questioned because of inappropriate analysis of N and Fe intermediates which can result in overestimated rates (Picardal 2012; Klueglein and Kappler 2013). Overall, the significance of Fe determining the relative importance of denitrification and DNRA in natural environments is currently poorly constrained.

The purpose of this study was to investigate the fate of NO_3^- in a eutrophic, seasonally hypoxic, N limited estuary. More specifically, we wanted to investigate how salinity and O_2 concentration affect the NO_3^- reduction pathways and how elevated availabilities of reduced S and Fe species affect the interplay between the different NO_3^- reducing pathways under anoxic conditions.

Methods

Sampling

Samples for the sediment incubations were collected from the Neuse River Estuary (NRE). The NRE is the largest subestuary of the lagoonal Albemarle-Pamlico Sound, which is the second largest estuarine complex in the lower USA. The average depth of the NRE is ~ 3.5 m and the astronomical tidal range is < 0.1 m (Luettich Jr. et al. 2000). Sediment composition in the NRE changes from sandy at the shoreline to muddy in mid-channel. Its watershed drains rapidly expanding agricultural (animal and row crop operations), urban (Raleigh–Durham Research Triangle), and industrial centers within the piedmont and coastal plain regions of North Carolina. The NRE has over the past several decades undergone anthropogenic eutrophication leading to increased phytoplankton production and bloom frequency (Paerl et al. 2010). The saltwater wedge extending from the downstream Pamlico Sound up into the estuary naturally decreases ventilation of the benthic waters and resultant hypoxia is a seasonal (spring through fall) feature of this estuary (Paerl et al. 1998; Fear et al. 2005).

Intact sediment cores (diameter 20 cm, height 50 cm), utilized for determining potential NO_3^- reduction rates, were collected with a custom-made coring device from the muddy mid-channel from one station (St70) in May 2016, and two stations (St30 and St70) in October 2016 and June 2017 (Fig. 1). Surface sediment (0–1 cm) for the slurry incubations was collected in May 2016 from St70. Temperature and salinity were recorded 50 cm above the sediment surface, using a YSI 6800 multi-probe sonde (YSI incorporated, Yellow Springs, OH, USA). The O_2, NO_2^- + NO_3^- (referred as NO_x^-) and NH_4^+ concentrations in the bottom water were determined by withdrawing a water sample from approximately 5 cm above the sediment surface in a core. The NO_x^- and NH_4^+ samples were filtered (prewashed 0.8/0.2-μm double filter syringe, Sarsted, Nümbrecht, Germany) and frozen at − 20 °C for subsequent flow-injection nutrient analysis (Lachat instruments, Loveland, CO, USA). Dissolved O_2 concentration was measured using the Winkler method (Grasshoff et al. 1999).

Intact Core Incubations

For the potential NO_3^- reduction measurements, each large core was sub-sampled using three or four smaller acryl plastic cores (diameter 2.5 cm, height 18 cm), so that there was approximately 5 cm of sediment and 13 cm of water in each subsample leaving no headspace in the cores. The sediment samples from different casts were randomized for the treatments in which they were enriched with potassium nitrate ($K^{15}NO_3^-$, 99% ^{15}N, Sigma–Aldrich, St. Louis, MO, USA (2016), and $K^{15}NO_3^-$, 99% ^{15}N, Cambridge Isotope Laboratories,

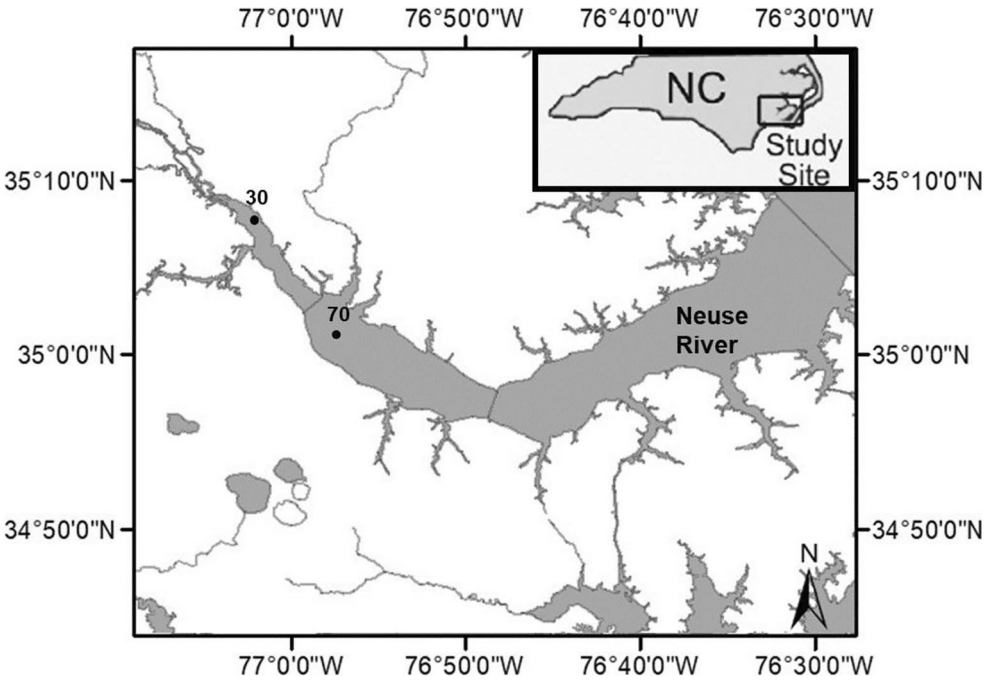

Fig. 1 Map of the Neuse Estuary in North Carolina, USA. The stations sampled in this study are marked as 30 and 70

Andover, MA, USA (2017)) to final concentration of 0, 40, 80, 120, and 160 μM $^{15}NO_3^-$ in the overlying water ($n = 4$ per $^{15}NO_3^-$ concentration). Thereafter, the cores were pre-incubated for 15 min prior to closing the caps. The cores without the tracer were sacrificed immediately at beginning of the incubation to calculate background $^{15}N_2$, $^{15}N_2O$, and $^{15}NH_4^+$ concentrations. The capped cores were incubated in darkness for 3–4 h at in situ temperature with magnetic stirring bars placed in the caps. After incubation, the sediment was mixed with the overlying water and allowed to stand until most sediment particles had settled (typically 5–15 min). A 12-ml water sample for isotopic analysis of N_2 and N_2O was withdrawn from the top of the core into a gas tight glass vial (Exetainer, Labco Scientific, High Wycombe, UK) containing 0.5 ml $ZnCl_2$ (100% w/v). The remaining core content was centrifuged (1500 rpm, 10 min) and the supernatant was filtered (prewashed 0.8/0.2-μm double filter syringe, Sarsted, Nümbrecht, Germany) and frozen at − 20 °C for subsequent and NH_4^+ and $^{15}NH_4^+$ analyses.

Slurry Incubations

To determine the effect of the availability of different electron donors on NO_3^- reduction rates, sediment-water slurries were prepared in May 2016 from sediment and water collected at St70. The slurry for the incubation experiments was comprised of the top 1 cm in the sediment cores and water collected directly above the sediment. The water and sediment were mixed at a 1:1 (vol:vol) ratio and purged with N_2 for 15 min to remove O_2 and background CO_2 and H_2S gases. Purging of the slurry was likely to increase the sample pH by 1–2 units due to CO_2 leaving the sample. However, St70 experiences pH changes in that range when the saltwater wedge is intruding in the estuary; thus, the microbes present in the sample are likely to experience similar changes naturally. After purging, the slurry was transferred into a glove bag and handled under a N_2 atmosphere until the incubation vials were capped. The slurry was divided into for four 1-l bottles for the following additions in the final concentration: (1) 1000 μM Na_2S (H_2S treatment); (2) 1000 μM Fe(II)SO_4 (Fe^{2+} treatment); (3) 1000 μM Na_2S + 1000 μM Fe(II)SO_4 (H_2S + Fe^{2+} treatment); (4) no additional electron donors (control treatment). All treatments received approximately 100 μM $K^{15}NO_3^-$. The treatment solutions were prepared in N_2 purged water and the Fe(II)SO_4 addition was verified to reduce the pH of the slurries by less than 0.5. The slurry from each treatment bottle was divided into 32 12-ml gas tight glass vials (Exetainer, Labco Scientific, High Wycombe, UK), resulting in a total of 128 samples. After preparation, the samples were incubated for approximately 6 h. Then four samples from each treatment were terminated for $^{15}N_2$ and $^{15}N_2O$ concentration measurements by creating a 4-ml He headspace and adding 100 μl of $ZnCl_2$ (100% w/v) to each sample. Simultaneously, incubations of four samples from each treatment were terminated by filtering the sample through prewashed 0.8/0.2-μM double filter syringes (Acrodisc, Pall Scientific, New York, NY, USA). Thereafter, samples were terminated every 6 h, until 24 h of incubation. The filtrate was analyzed within few hours for NO_3^- and NO_2^-, (Fawcett and Scott 1960; Miranda et al. 2001) and the rest of the samples were frozen at − 20 °C and analyzed later for NH_4^+ and $^{15}NH_4^+$ concentrations.

^{15}N Analyses

For the $^{15}N_2$ and $^{15}N_2O$ gas samples, a 4 ml helium (He) headspace was created immediately before analysis and samples withdrawn from the headspace were analyzed with a ThermoScientific GasBench + Precon gas concentration system interfaced to a ThermoScientific Delta V Plus isotope-ratio mass spectrometer (ThermoScientific, Bremen, Germany) at the University of California Davis Stable Isotope Laboratory (Davis, CA, USA) (May 2016) and with Isoprime100 IRMS coupled to an Isoprime TraceGas preconcentration unit (Elemental Analysensysteme GmbH, Langenselbold, Germany) at the University of Jyväskylä (Jyväskylä, Finland) (October 2016 and June 2017).

The $^{15}NH_4^+$ analysis was modified from Sigman et al. (1997) and Holmes et al. (1998). First, NH_4^+ concentrations of the samples were determined according Fawcett and Scott (1960) to ensure that a minimum of 10 μM NH_4^+ was available for the extraction. Then, 10 ml of sample was placed in a 20-ml HDPE scintillation vial (Wheaton, Millville, NJ, USA) and the salinity of the samples was adjusted to 30 with sodium chloride (NaCl). Thereafter, 100 mg of magnesium oxide (MgO) was added to each sample. pH was measured after the addition of MgO to ensure that it was optimal (~ 10) pH for the conversion of NH_4^+ to NH_3. The liberated NH_3 was collected in diffusion packets which were constructed by pipetting 30 μl of 2.5 M potassium bisulfate ($KHSO_4$) on to a fiberglass filter (Whatman, GF/D, diameter 5 mm, Whatman, Maidstone, Kent, UK) that was placed between two pieces of Teflon tape. The diffusion packets were added prior to MgO addition to minimize NH_3 escaping before closing the vials. The vials were incubated for 3 days at + 37 °C on a shaker table (150 rpm). Then, the diffusion packets were removed from the vials and placed in a desiccator under a sulfuric acid (H_2SO_4) atmosphere to dry. After 2 days, the packets were disassembled, and the fiberglass filters were packed into silver foil cups (Elemental Microanalyses Ltd., Toft, Cambridge, UK). The isotopic ratio of the extracted N was analyzed using Thermo Finnigan Delta V plus (Thermo Scientific, Waltham, MA, USA) at the University of Eastern Finland (Kuopio, Finland).

Calculations and Statistics

Our initial aim was to measure in situ NO_3^- reduction rates with the isotope pairing method (IPT; Nielsen 1992, Christensen et al. 2000, Risgaard-Petersen et al. 2003, 2004, Master et al. 2005). However, two problems arose during the measurements: (1) The concentration of ^{15}N-labelled N species did not always linearly increase with the $^{15}NO_3^-$ concentration (supplementary figure) and (2) the O_2 concentration in the cores during all sampling times was so low that although the incubation time was kept as short as possible, the cores were nearly anoxic by the end of the incubation. These artifacts violate the fundamental assumptions behind the IPT (Nielsen 1992), and calculation of reliable in situ NO_3^- reduction rates was impossible. Therefore, we calculated only the potential NO_3^- reduction rates be averaging the ^{15}N production rates from all $^{15}NO_3^-$ concentrations.

Potential N_2 production is the average of excess $^{15}N_2$ ($p^{29}N_2 + 2 \times {}^{30}N_2$), potential N_2O production is the average of excess $^{15}N_2O$ ($p^{45}N_2O + 2 \times p^{46}N_2O$), and potential DNRA is the average excess $^{15}NH_4^+$ production. Because in June 2017 there was an increasing trend in the $^{15}N_2$ production with the $^{15}NO_3^-$ concentration, the potential during that sampling time provides only a minimum estimate and the actual potentials might be higher (supplementary figure). The differences in rates measured in the core samples were tested by using Whitney–Mann U test. The correlations between the potential rates and environmental parameters were determined by using non-parametric correlation analysis.

The NO_3^- consumption and NO_2^-, $^{15}N_2$, $^{15}N_2O$, and $^{15}NH_4^+$ production rates were calculated from liner regression analysis between the N concentration of different N-species and time. Rates were considered significant at $p = 0.05$. The comparison between the rates was done by using two-way ANOVA.

Results

Environmental Conditions

Both stations were hypoxic during all sampling times. However, there was always a small amount O_2 detected, except in Oct 2016 at st70 when the odor of H_2S was detected in the bottom water and in May 2017 at St30 when O_2 was at the detection limit (~ 3 μmol l^{-1}) of the Winkler method (Table 1).

In May 2016, the bottom water salinity was at its lowest at St70, most likely due to excessive rainfall and elevated freshwater runoff which pushed the salt wedge towards the outlet of the estuary. In October 2016, the bottom water salinity at St70 was higher compared with May; however, the saltwater wedge did not reach deep into the estuary and the salinity at St30 was 0. In June 2017, when the river flow had remained low and the saltwater wedge intruded deep into the estuary, the bottom water salinity was 12 at St70 and 10 at St30 (Table 1). The bottom water NO_x^- concentration was always higher at St30 than at St70, but the opposite was true for NH_4^+ (Table 1).

Potential Denitrification and DNRA Rates Measured on the Intact Cores

There was no evidence of anammox based on the IPT calculations (Risgaard-Petersen et al. 2003, 2004); hence, most N_2 must have originated from denitrification. Occasionally 1–2

Table 1 The average NH_4^+, NO_x^-, and O_2 concentrations measured 5 cm above the sediment surface. Temperature and salinity were measured 50 cm above the sediment. H_2S, H_2S present in the water; B/D, below detection; SD, standard deviation

	O_2 μmol l^{-1}	NH_4^+ μmol l^{-1}	NO_x^- μmol l^{-1}	Temp (°C)	Salinity	% of DNRA from total NO_3^- reduction (SD)	% of N_2O from total denitrification (SD)
St70							
May 2016	37.5	1.7	0.3	26.6	4.9	63.5 (14.2)	13.3 (13.2)
October 2016	H_2S	33.1	1.3	26.1	10.8	88.9 (11.1)	100.0 (0.0)
June 2017	40.6	39.8	3.9	20.2	11.5	65.8 (10.8)	11.1(9.6)
St30							
October 2016	34.4	11.1	18.4	24.0	0.1	90.0 (15.1)	47.5(38.4)
June 2017	B/D	19.1	6.1	19.9	9.9	78.0 (22.7)	29.9 (29.3)

samples were lost during sample processing, and consequently there was 14–16 samples analyzed per station per sampling time. During all sampling times, the potential DNRA rates were equal (June 2017, St30, $n = 16$, $p = 0.861$) or significantly higher (May 2016, St70, $n = 15$, $p = 0.050$; October 2016, St70, $n = 15$, $p = 0.000$; October 2016, St30, $n = 14$, $p = 0.000$; June 2017, St70, $n = 16$, $p = 0.008$) than the potential denitrification ($N_2O + N_2$) rates at both stations. The total NO_3^- reduction rates (denitrification + DNRA) were always significantly lower at St30 than at St70 (October 2016, $n = 15$, $p = 0.000$; June 2017, $n = 16$, $p = 0.000$) (Fig. 2). In October 2016, potential N_2 production was detected in only in seven samples at St70 and at twelve samples at St70, while the rest were below the detection limit. $^{15}N_2O$ production was detected in 12 samples St70 and at all samples at St30. Where denitrification was detected, over 50% of it was N_2O (Table 1). However, potential DNRA was still proceeding at measurable rates at both stations. There was no significant difference in denitrification and DNRA rates between May 2016 and June 2017 ($n = 15$ in May 2016 St70 and $n = 16$ in June 2017 St70, $p = 0.545$ for denitrification and $p = 0.866$ for DNRA) (Fig. 2). There were no statistically significant correlations ($p < 0.05$) between the production of ^{15}N-labelled products and environmental parameters (O_2, temperature and salinity) in the core samples.

Potential Denitrification and DNRA Rates Measured from Slurry Samples

The addition of 1 mM H_2S increased the $^{15}NO_3^-$ consumption rates, although not significantly, when compared with the control samples and with samples that had $H_2S + Fe^{2+}$ (Table 2). Although the total $^{15}N_2$ concentration remained lower than in the control samples, it was still increasing steadily over the entire incubation period (Fig. 3). There was also a steady increase in the $^{15}NH_4^+$ concentration and the total $^{15}NH_4^+$ production rates were significantly higher in the samples that were amended with H_2S compared with all other treatments

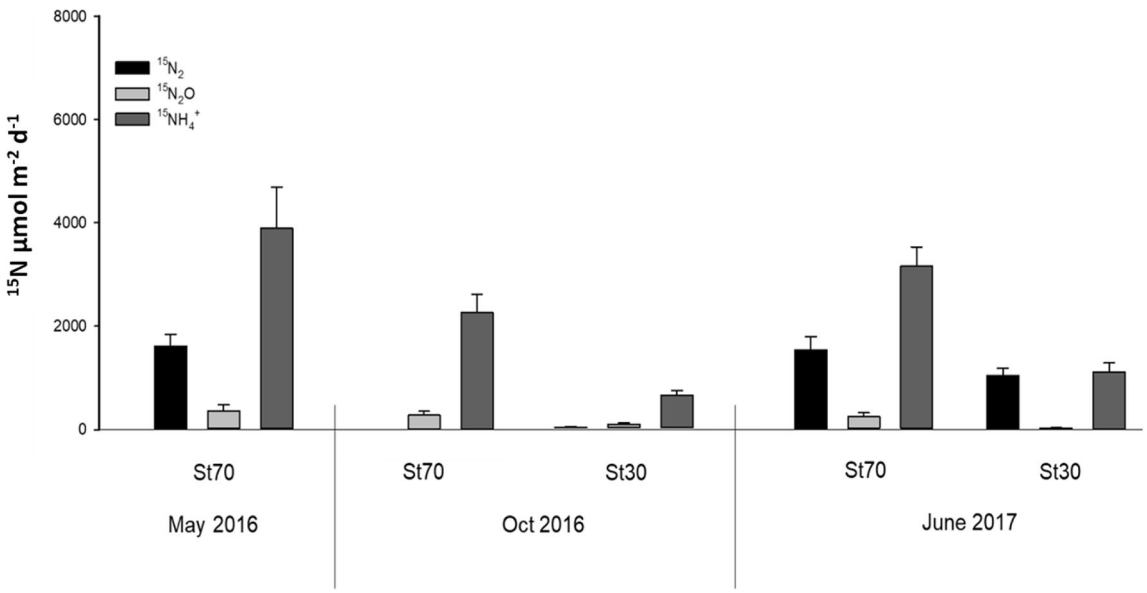

Fig. 2 The denitrification ($^{15}N_2$ and $^{15}N_2O$) and DNRA ($^{15}NH_4^+$) potentials measured from the intact sediment cores

Table 2 The N consumption and production rates calculated from regression analysis between concentrations of N species and time. Linearly significant regressions ($p \leq 0.05$) are presented in italics

Treatment	NO_3^- μmol N l^{-1} day^{-1} (SE)	NO_2^- μmol N l^{-1} day^{-1} (SE)	$^{15}N_2$ μmol N l^{-1} day^{-1} (SE)	$^{15}N_2O$ μmol N l^{-1} day^{-1} (SE)	$^{15}NH_4^+$ μmol N l^{-1} day^{-1} (SE)
First three time points					
H_2S	*− 32.1 (8.2)* *n = 12; p = 0.00*	0.3 (0.2) n = 12; p = 0.06	*12.6 (5.7)* *n = 12; p = 0.05*	0.5 (0.9) n = 12; p = 0.61	*14.1 (4.7)*[3] *n = 11; p = 0.01*
Fe^{2+}	*− 155.0 (22.1)*[1] *n = 12; p = 0.00*	− 0.2 (0.4) n = 12; p = 0.60	− 8.2 (25.4) n = 12; p = 0.75	*2.2 (1.0)* *n = 12; p = 0.05*	*4.6 (1.7)* *n = 11; p = 0.02*
$H_2S + Fe^{2+}$	*− 36.2 (10.2)* *n = 12; p = 0.01*	− 2.1 (1.8) n = 12; 0.27	*16.0 (5.9)* *n = 12; p = 0.02*	− 0.6 (0.8) n = 12; p = 0.51	− 0.4 (2.5) n = 11; p = 0.87
Control	*−23.8 (4.6)* *n = 12; p = 0.00*	*4.7 (1.9)* *n = 12; p = 0.03*	*26.9 (5.2)*[2] *n = 11; p = 0.02*	0.6 (2.8) n = 12; p = 0.83	0.8 (1.0) n = 12; p = 0.42
Last time point					
H_2S	− 36.5 (17.9) n = 4; p = 0.08	*0.8 (0.3)*[4] *n = 4; p = 0.04*	21.9 (12.4) n = 4; p = 0.12	− 0.7 (0.1) n = 4; p = 0.50	− 1.7 (15.0) n = 4; p = 0.91
Fe^{2+}	− 69.7 (43.9) n = 3; p = 0.16	*− 2.6 (1.0)* *n = 3; p = 0.04*	17.4 (13.0) n = 4; p = 0.23	*− 18.4 (1.6)*[6] *n = 4; p = 0.00*	*− 5.1 (2.1)* *n = 4; p = 0.06*
$H_2S + Fe^{2+}$	− 23.8 (19.1) n = 3; p = 0.27	*− 13.7 (2.8)*[5] *n = 4; p = 0.00*	*18.7 (6.7)* *n = 4; p = 0.03*	*− 8.4 (2.0)* *n = 4; p = 0.01*	4.2 (6.1) n = 4; p = 0.51
Control	*− 35.2 (11.1)* *n = 3; p = 0.02*	*− 16.0 (4.8)* *n = 4; p = 0.02*	*39.9 (12.9)* *n = 4; p = 0.02*	*− 8.2 (3.7)* *n = 4; p = 0.07*	3.27 (3.2) n = 4; p = 0.42

[1] Significantly higher NO_3^- consumption compared with other treatments ($p = 0.00$)

[2] Higher $^{15}N_2$ production compared with H_2S-treated samples at $p = 0.08$

[3] Higher $^{15}NH_4^+$ production rate than in Fe^{2+}-treated samples at $p = 0.07$

[4] Significantly higher than the other treatments ($p = 0.00$–0.05)

[5] Significantly lower than Fe^{2+}-treated samples ($p = 0.03$)

[6] Significantly lower than $H_2S + Fe^{2+}$-treated samples ($p = 0.02$) and lower than the control samples at $p = 0.06$

(Table 2). However, H_2S did not inhibit denitrification completely (Table 2, Fig. 3).

Amendment of Fe^{2+} stimulated the NO_3^- consumption a nearly sixfold compared with the control samples (Table 2, Fig. 3). However, the sink of NO_3^- is unclear because after the initial increases in the concentrations of $^{15}N_2$ and $^{15}NH_4^+$, their concentrations remained steady ($^{15}N_2$) or increased only moderately ($^{15}N_2O$, $^{15}NH_4^+$) over the entire incubation period, although NO_3^- consumption continued at a high rate (Table 2, Fig. 3).

The samples which were amended with both H_2S and Fe^{2+} had slightly lower $^{15}N_2$ production rates and slightly higher NO_3^- consumption rates when compared with the control samples. This and the high NO_3^- consumption in the Fe^{2+}-amended samples indicate that Fe^{2+} stimulates NO_3^- consumption regardless whether H_2S is present or not (Table 2, Fig. 3).

The NO_2^- concentrations remained low in samples that were treated with either H_2S or Fe^{2+}. However, when H_2S and Fe^{2+} were added in equal concentrations, NO_2^- concentration was higher than in the samples treated with only H_2S or Fe^{2+} but lower than in the control samples. Interestingly, concentrations and production rates of N_2O followed NO_2^- concentrations and production rates and they all decreased at the last sampling point, except in the H_2S treatments where the NO_3^- concentration was approximately double as high compared with other treatments (Table 2, Fig. 3). The $^{15}NH_4^+$ product increased, although not significantly, simultaneously to the decrease in NO_2^- concentration at the last sampling point in the control samples and $H_2S + Fe^{2+}$-treated samples (Fig. 3).

Discussion

NO_3^- Reduction Rates in the Intact Cores

Overall, potential denitrification rates measured in the NRE were on the lower end of the range of average in situ denitrification rates in temperate coastal sediments (1.2–5 mmol m^2 day^{-1}; Seitzinger 1988) but within the same range (0–6600 μM N m^{-2} day^{-1}) previously measured in the NRE by Fear et al. (2005). The low rates in this study can be explained by sampling during warm months when hypoxia is present, which is when Fear et al. (2005) also measured the lowest denitrification rates.

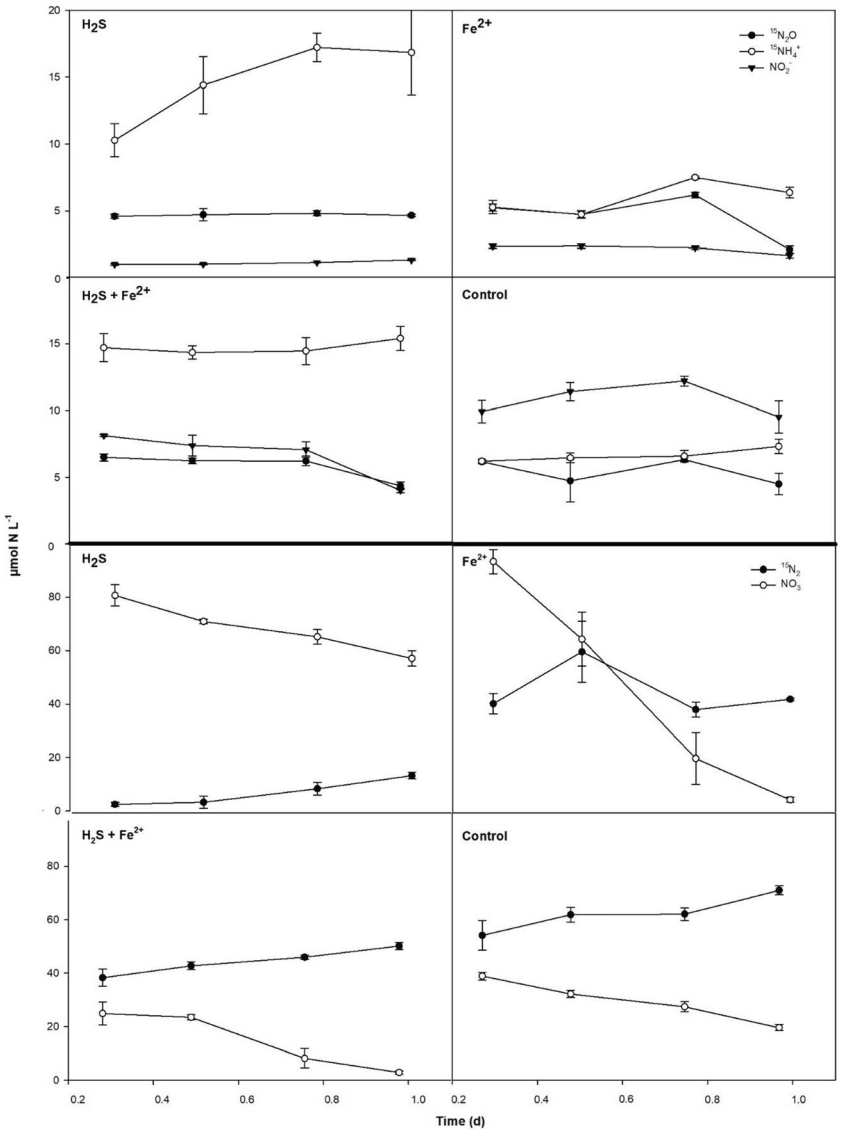

Fig. 3 Concentrations of $^{15}N_2$, $^{15}N_2O$, $^{15}NH_4^+$, NO_2^-, and NO_3^- over the incubation period from slurry samples that were amended with different electron donors. The control samples had no added electron donors. All samples initially contained approximately 100 μM $^{15}NO_3^-$

Although denitrification is an anoxic process, there typically is a positive correlation between denitrification rates and O_2 concentration because nitrification, which provides NO_3^- for denitrification, is stimulated by the availability of O_2 (Jenkins and Kemp 1984; Kemp et al. 1990). Since we only measured potentials, where denitrification is not limited by the availability of NO_3^-, we expected to find a negative correlation between denitrification rates and O_2 concentration. However, no such correlation was found, and this may be because under hypoxia the presence of H_2S, rather than the negligible availability of O_2, is likely to be the key regulating factor for denitrification.

N_2O production in core samples collected in October 2016 was on the higher end of measured sedimentary N_2O fluxes in estuarine environments (Murray et al. 2015 and the references there in). This can be partially explained by it being a potential rather than in situ rate since there was more NO_3^- available than under naturally occurring conditions. Presence of H_2S in the bottom water clearly favored N_2O production over N_2 production, since 99% of end product of denitrification was N_2O (Table 1). This is consistent with the early findings of Sørensen et al. (1980) reporting inhibition of N_2O reduction causing accumulation of N_2O in the presence of H_2S.

The potential DNRA rates measured at St70 are comparable with DNRA rates measured in the other estuaries in the southern USA (0–2.4 mmol N m^{-2} day^{-1}; Gardner et al. 2006); (0–8.2 mmol N m^{-2} day^{-1}; Giblin et al. 2010) as well as rates measured in sulfide-rich sediments in Denmark (0–6.5 mmol N day^{-1}, Christensen et al. 2000). At St30, potential DNRA rates were substantially lower but still comparable with DNRA rates measured in periodically anoxic Baltic Sea sediments (0.03–1.1 mmol N m^{-2} day^{-1}; Jäntti and Hietanen 2012). Surprisingly, there was also no correlation between the DNRA and O_2 concentration, and the highest DNRA rates

were measured under conditions when little O_2 was available (May 2016). This may be because NO_3^- reduction to NO_2^-, the first step of DNRA, is suggested to be also be driven by denitrifying bacteria (Canfield et al. 2005) which can be inhibited by H_2S. Hence, the DNRA rates were probably limited by the NO_2^- availability. It appears that if H_2S is present near denitrification layer, the overall NO_3^- reduction rates are lower than in conditions when H_2S is not present. However, the lowest denitrification to DNRA ratio was found when H_2S was present in the bottom water (Oct 2016) suggesting that the presence of H_2S inhibited denitrification relatively more than DNRA.

Salinity did not correlate with any of the ^{15}N production rates, although increases in salinity have been linked to stimulation of DNRA (Gardner et al. 2006; Giblin et al. 2010). Consequently, it appears that in the NRE, the duration of hypoxia, rather than salinity or O_2 availability, determines the dominance of DNRA over denitrification.

NO_3^- Reduction Rates in the Sediment Slurry Samples

In the slurry samples, the slopes of N_2 production and NO_3^- consumption proceeded steadily but in opposite directions in the control and $H_2S + Fe^{2+}$ treatments, indicating presence of denitrification. Similar $^{15}N_2$ production and NO_3^- consumption pattern between the control and $H_2S + Fe^{2+}$ treatments can be explained by H_2S chemically reacting with Fe^{2+} and forming iron sulfide (FeS), which is a relatively stable compound and does not act as an electron donor for either DNRA or denitrification (Brunet and Garcia-Gil 1996). However, the $^{15}NH_4^+$ concentration was higher in the $H_2S + Fe^{2+}$-treated samples compared with the control samples and it appears that presence of additional electron donors caused a higher percentage of NO_3^- to be converted to NH_4^+ over the entire incubation period. Because there was no NO_2^- accumulation and substantial $^{15}NH_4^+$ accumulation in the $H_2S + Fe^{2+}$-treated samples, it is likely that the additional electron acceptors stimulated NO_2^- reduction, the end product of which is NH_4^+. The simultaneously elevated concentrations of NO_2^- and N_2O in nearly all treatments are in line with the results from wastewater treatment facilities where high N_2O production during the denitrification phase has been linked with elevated NO_2^- concentrations, although the explanation for this relationship is not clear (Kampschreur et al. 2009).While NO_2^- and N_2O concentrations began to decrease during the last measurement time, the $^{15}NH_4^+$ concentration began to increase, although the increase was not linearly significant, suggesting that DNRA has a higher affinity for NO_2^- than denitrification, similar to results of Kraft et al. (2014). However, the opposite has been observed in chemostat experiments (van den Berg et al. 2017), suggesting that the dominant NO_2^- reduction pathway is also dependent on NO_2^- reducing microbial community composition.

In the H_2S-treated slurries, there was a steady increase in $^{15}N_2$, suggesting that denitrifying microbes were still reducing NO_3^-, although at rates lower than the controls and almost equal proportions of NO_3^- were reduced to N_2 and NH_4^+. This was expected, since stimulation of DNRA under elevated H_2S concentrations has been previously demonstrated in several studies (Høgslund et al. 2009; Schutte et al. 2018; An and Gardner 2002; McCarthy et al. 2008; Jäntti and Hietanen 2012; Bernard et al. 2015; Murphy et al. 2020), as well as in our core incubations, where the highest DNRA to denitrification ratio was observed when the bottom water contained H_2S in October 2016. However, the NO_3^- concentrations remained higher in the H_2S-treated samples than in the control and $H_2S + Fe^{2+}$-treated samples, suggesting that H_2S overall inhibits NO_3^- reduction, particularly immediately after it becomes present. This was indicated by much lower decrease in the NO_3^- concentration at the first 6 h of incubation in the H_2S-treated samples when compared with the control samples. Interestingly, the N_2O accumulation in the H_2S-treated samples was not substantially higher than in the control samples, although N_2O accumulation was observed in the intact cores in presence of H_2S. This could be explained by slurries being in a closed incubation system where intermediates, such as N_2O, cannot escape from the active site (sediment surface) during the incubation, unlike in the intact cores and consequently the intermediates in denitrification/DNRA were consumed at the rate which they were formed.

The effect of Fe^{2+} on N cycling is not yet well understood because it is challenging to separate the roles of abiotic and biotic processes since they can combine, even within a single organism (Picardal 2012; Melton et al. 2014; Ionescu et al. 2015). Also, most studies have been done by using microbial cultures, and the role of micro-organisms oxidizing Fe^{2+} with NO_3^- in natural environments is currently poorly known. In the slurry samples, there was a rapid accumulation of $^{15}N_2$ at beginning of the incubation in Fe^{2+}-treated samples. However, the concentration of $^{15}N_2$ did not change after the initial increase; hence, denitrification was quickly brought to a halt. The rapid decrease in N_2 formation in the Fe^{2+}-treated samples could be caused by Fe^{2+} reacting with the organic carbon compounds present in the sediment producing poorly degradable compounds (Lalonde et al. 2012; Shields et al. 2016), and thus the low availability of labile organic carbon limited heterotrophic denitrification shortly after Fe^{2+} was introduced. Fe^{2+} can also disturb intracellular electron transport (Carlson et al. 2012) that inhibits denitrification rates and could explain the non-linear increase of $^{15}N_2$ in the Fe^{2+}-treated slurries.

The low $^{15}NH_4^+$ formation in the Fe^{2+}-treated samples was unexpected as several studies have demonstrated that Fe^{2+} stimulates microbe-mediated DNRA (Robertson et al. 2016; Robertson and Thamdrup 2017; Kessler et al. 2018; Kessler et al. 2019) and abiotic NO_3^- reduction to NH_4^+ (Hansen et al.

1994; Hansen et al. 1996; Guerbois et al. 2014). Hence, DNRA in sediments of at St70 appears to be driven by H_2S rather than Fe^{2+}. This could be because the hypoxia is severe and long-lasting in the NRE (Buzzelli et al. 2002), causing H_2S to rise regularly to the sediment surface and thus favoring microbes that can tolerate and utilize H_2S in their metabolism. The reports of Fe^{2+} stimulating DNRA are mainly from sediments where free H_2S is not available due to Fe^{2+} binding the free sulfides (Robertson et al. 2016; Robertson and Thamdrup 2017; Kessler et al. 2018). Also, there was no visible sign of the presence of cable bacteria which have been shown to promote DNRA through Fe-sulfide dissolution (Kessler et al. 2019).

There was the steep negative slope of NO_3^- concentration in the Fe^{2+}-treated slurries and the NO_3–N was not recovered from the N_2, N_2O, or from the DIN pools. One possible explanation for the disappearance of NO_3^- could be formation of nitric oxide (NO), which has been reported in the presence of Fe^{2+} (Carlson et al. 2012 and references therein). Since NO is highly volatile, it can be released immediately after opening the incubation vials. Also, because NO is highly reactive with metal oxides and formation of metal nitrosyls during the incubation, this cannot be excluded. It appears that additional chemical reactions between NO_3^- and Fe^{2+} can play a significant role in the sedimentary coastal N cycling and deserve further investigations.

Lack of NO_2^- accumulation in the Fe^{2+}- and H_2S-treated samples indicates that the additional electron acceptors particularly stimulate NO_2^- reduction rates. In the H_2S-treated samples, NO_2^- was likely to be reduced to NH_4^+, whereas in the Fe^{2+}-treated samples, the end product of NO_2^- reduction is not clear. Both NO_2^- and Fe^{2+} are highly reactive, and one of the best documented reactions between NO_2^- and Fe^{2+} is the formation of N_2O (Moraghan and Buresh 1977). However, neither N_2O production nor changes in concentrations of the other measured N species match the NO_3^- consumption rates. Hence, unmeasured processes, such as NO formation, seem more likely.

Conclusions

Based on the results of this and other experiments, we conclude that the length of hypoxia has a substantial effect on the N cycling processes in carbon and SO_4^{2-} rich sediments and that the role of Fe^{2+} has to investigated more thoroughly in hypoxic estuarine sediments where H_2S accumulation occurs. When O_2 is present in the sediment surface (Fig. 4A), nitrification proceeds at the rate which NH_4^+ is produced by mineralization. There is no NH_4^+ release in the bottom water because nitrification efficiently oxidizes the produced NH_4^+, and denitrification is tightly coupled to nitrification. The DNRA rates are low because in the absence of H_2S, aerobic heterotrophy dominates, and DNRA microbes cannot compete with denitrification because the quality of organic carbon available for anaerobic processes, after intensive aerobic processes, is low (Kraft et al. 2014). When hypoxia first settles in (Fig. 4B), nitrification proceeds at high rates because nitrification can tolerate microaerophilic conditions (Laanbroek and Gerards 1993; Jäntti et al. 2018) although the end product of nitrification can switch to N_2O (Kalvelage et al. 2011). The denitrification rates increase because denitrification is stimulated by decreasing O_2 concentrations (Hietanen and Lukkari 2007).

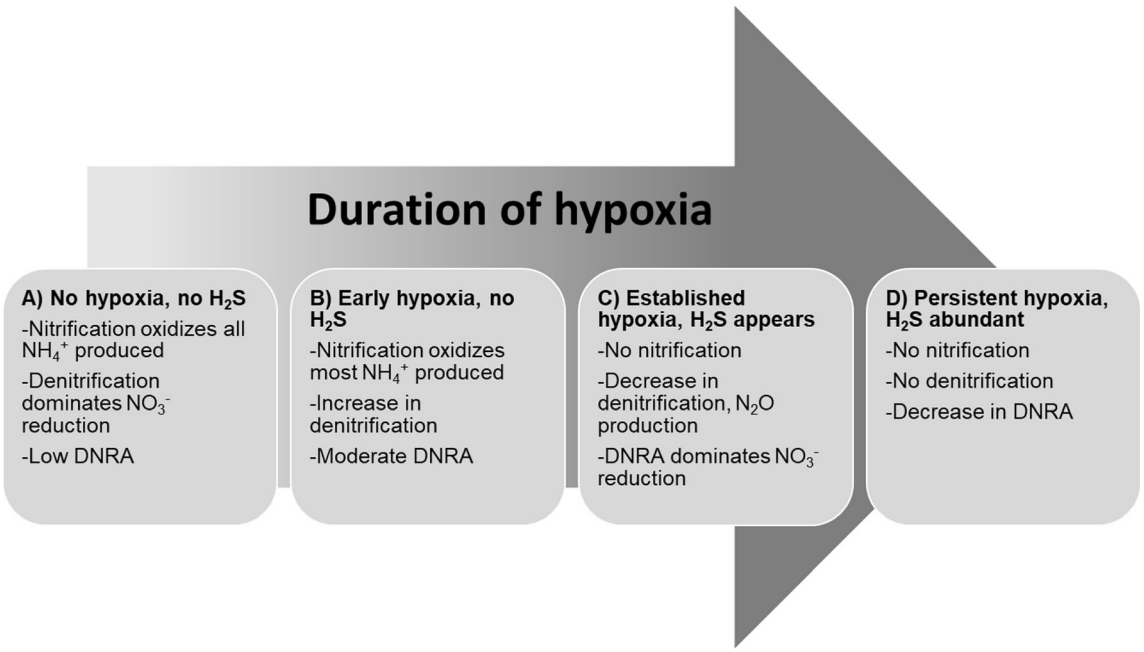

Fig. 4 The effect of length of hypoxia on NO_3^- reduction in eutrophic SO_4^{2-}-rich estuarine sediments

At this stage, availability of H_2S near the sediment surface is still low, and consequently chemolithotrophic DNRA rates remain moderate. When hypoxia is established (Fig. 4C), H_2S reaches sediment surface and nitrification ceases because it does not tolerate H_2S (Joye and Hollibaugh 1995). Denitrification rates decrease and the end product of denitrification changes from N_2 to N_2O. At the same time, DNRA begins to dominate NO_3^- reduction. During persistent hypoxia (Fig. 4D), H_2S reaches bottom water, and there is no nitrification and only very little denitrification. DNRA rates also decrease because of low NO_2^- availability.

Acknowledgments We thank members of the Paerl Lab, including B. Abare, J. Braddy, K. Rossignol, and R. Sloup, for assistance during the incubations and sample analysis. We also thank S. Jokinen (UEF) for assistance during the IRMS analyses and C. Treat (UEF) for help with the map.

Funding Information Open access funding provided by University of Eastern Finland (UEF) including Kuopio University Hospital. This research was funded by the Academy of Finland (grant nos. 275127 and 307331 (Jäntti), 310302 (Aalto)) and joint funding by Olvi Foundation, Jenny and Antti Wihuri foundation, and Saastamoinen funding (Jäntti). The works were partially supported by the US National Science Foundation (DEB 1240851; OCE 1705972), The North Carolina Dept. of Environmental Quality and US National Fish and Wildlife Federation (Project 8020.16.053916: ModMon Program), the Lower Neuse Basin Association, NC Sea Grant, and the UNC Water Resources Research Institute.

References

An, S., and W.S. Gardner. 2002. Dissimilatory nitrate reduction to ammonium (DNRA) as a nitrogen link, versus denitrification as a sink in a shallow estuary (Laguna Madre/Baffin Bay, Texas). *Marine Ecology Progress Series* 237: 41–50. https://doi.org/10.3354/meps237041.

Bernard, R.J., B. Mortazavi, and A.A. Kleinhuizen. 2015. Dissimilatory nitrate reduction to ammonium (DNRA) seasonally dominates NO_3^- reduction pathways in an anthropogenically impacted subtropical coastal lagoon. *Biogeochemistry* 125 (1): 47–64. https://doi.org/10.1007/s10533-015-0111-6.

Breitburg, D., L.A. Levin, A. Oschlies, M. Grégoire, F.P. Chavez, D.J. Conley, V. Garçon, D. Gilbert, D. Gutiérrez, K. Isensee, G.S. Jacinto, K.E. Limburg, I. Montes, S.W.A. Naqvi, G.C. Pitcher, N.N. Rabalais, M.R. Roman, K.A. Rose, B.A. Seibel, M. Telszewski, M. Yasuhara, and J. Zhang. 2018. Declining oxygen in the global ocean and coastal waters. *Science* 359 (6371): eaam7240. https://doi.org/10.1126/science.aam7240.

Brettar, I., and G. Rheinheimer. 1991. Denitrification in the Central Baltic: evidence for H_2S-oxidation as motor of denitrification at the oxic-anoxic interface. *Marine Ecology Progress Series* 77: 157–169.

Brunet, R.C., and L.J. Garcia-Gil. 1996. Sulfide-induced dissimilatory nitrate reduction to ammonia in anaerobic freshwater sediments. *FEMS Microbiology Ecology* 21 (2): 131–138. https://doi.org/10.1111/j.1574-6941.1996.tb00340.x.

Buresh, R.J., and J.T. Moraghan. 1976. Chemical reduction of nitrate by ferrous iron 1. *Journal of Environmental Quality* 5 (3): 320–325. https://doi.org/10.2134/jeq1976.00472425000500030021x.

Buzzelli, C.P., S.P. Powers, R.A. Luettich Jr., J.E. McNinch, C.H. Peterson, J.L. Pinckney, and H.W. Paerl. 2002. Estimating the spatial extent of bottom water hypoxia and benthic fishery habitat degradation in the Neuse River Estuary, NC. *Mar Ecol Progr Ser* 230: 103–112.

Canfield, D.E. 1989. Sulfate reduction and oxic respiration in marine sediments: implications for organic carbon preservation in euxinic environments. *Deep Sea Res A* 36 (1): 121–138.

Canfield, D.E., E. Kristensen, and B. Thamdrup. 2005. *Aquatic geomicrobiology*. New York: Academic Press.

Carlson, H.K., I.C. Clark, R.A. Melnyk, and J.D. Coates. 2012. Toward a mechanistic understanding of anaerobic nitrate-dependent iron oxidation: balancing electron uptake and detoxification. *Frontiers in Microbiology* 3: 57. https://doi.org/10.3389/fmicb.2012.00057.

Christensen, P.B., S. Rysgaard, N.P. Sloth, T. Dalsgaard, and S. Schwærter. 2000. Sediment mineralization, nutrient fluxes, denitrification and dissimilatory nitrate reduction to ammonium in an estuarine fjord with sea cage trout farms. *Aquatic Microbial Ecology* 21: 73–84. https://doi.org/10.3354/ame021073.

Dalsgaard, T., B. Thamdrup, and D.E. Canfield. 2005. Anaerobic ammonium oxidation (anammox) in the marine environment. *Research in Microbiology* 156 (4): 457–464. https://doi.org/10.1016/j.resmic.2005.01.011.

Diaz, R.J., and R. Rosenberg. 1995. Marine benthic hypoxia: a review of its ecological effects and the behavioural responses of benthic macrofauna. *Oceanography and Marine Biology* 33: 245–303.

Diaz, R.J., and R. Rosenberg. 2008. Spreading dead zones and consequences for marine ecosystems. *Science* 321 (5891): 926–929. https://doi.org/10.1126/science.1156401.

Dong, L.F., M.N. Sobey, C.J. Smith, I. Rusmana, W. Phillips, A. Stott, A.M. Osborn, and D.B. Nedwell. 2011. Dissimilatory reduction of nitrate to ammonium, not denitrification or anammox, dominates benthic nitrate reduction in tropical estuaries. *Limnology and Oceanography* 56 (1): 279–291. https://doi.org/10.4319/lo.2011.56.1.0279.

Fawcett, J.K., and J. Scott. 1960. A rapid and precise method for the determination of urea. *Journal of Clinical Pathology* 13 (2): 156–159.

Fear, J.M., S.P. Thompson, T.E. Gallo, and H.W. Paerl. 2005. Denitrification rates measured along a salinity gradient in the eutrophic Neuse River Estuary, North Carolina, USA. *Estuaries* 28 (4): 608–619. https://doi.org/10.1007/BF02696071.

Gardner, W.S., M.J. McCarthy, S. An, D. Sobolev, K.S. Sell, and D. Brock. 2006. Nitrogen fixation and dissimilatory nitrate reduction to ammonium (DNRA) support nitrogen dynamics in Texas estuaries. *Limnology and Oceanography* 51 (1part2): 558–568. https://doi.org/10.4319/lo.2006.51.1_part_2.0558.

Giblin, A.E., N.B. Weston, G.T. Banta, J. Tucker, and C.S. Hopkinson. 2010. The effects of salinity on nitrogen losses from an oligohaline estuarine sediment. *Estuaries and Coasts* 33 (5): 1054–1068. https://doi.org/10.1007/s12237-010-9280-7.

Grasshoff, K., K. Kremling, and M. Ehrhardt. 1999. *Methods of seawater analysis*. 3rd ed. Weinheim: Verlag Chemie GmbH.

Guerbois, D., G. Ona-Nguema, G. Morin, M. Abdelmoula, A.M. Laverman, J.M. Mouchel, K. Barthelemy, F. Maillot, and J. Brest. 2014. Nitrite reduction by biogenic hydroxycarbonate green rusts: evidence for hydroxy-nitrite green rust formation as an intermediate reaction product. *Environmental Science & Technology* 48 (8): 4505–4514. https://doi.org/10.1021/es404009k.

Hannig, M., G. Lavik, M.M.M. Kuypers, D. Woebken, W. Martens-Habbena, and K. Jürgens. 2007. Shift from denitrification to anammox after inflow events in the Central Baltic Sea. *Limnology and Oceanography* 52 (4): 1336–1345. https://doi.org/10.4319/lo.2007.52.4.1336.

Hansen, H.C.B., O.K. Borggaard, and J. Sørensen. 1994. Evaluation of the free energy of formation of Fe (II)-Fe (III) hydroxide-sulphate (green rust) and its reduction of nitrite. *Geochimica et Cosmochimica Acta* 58 (12): 2599–2608. https://doi.org/10.1016/0016-7037(94)90131-7.

Hansen, H.C.B., C.B. Koch, H. Nancke-Krogh, O.K. Borggaard, and J. Sørensen. 1996. Abiotic nitrate reduction to ammonium: key role of green rust. *Environmental Science & Technology* 30 (6): 2053–2056. https://doi.org/10.1021/es950844w.

Hietanen, S., and J. Kuparinen. 2008. Seasonal and short-term variation in denitrification and anammox at a coastal station on the Gulf of Finland, Baltic Sea. *Hydrobiologia* 596 (1): 67–77.

Hietanen, S., and K. Lukkari. 2007. Effects of short-term anoxia on benthic denitrification, nutrient fluxes and phosphorus forms in coastal Baltic sediment. *Aquatic Microbial Ecology* 49: 293–302. https://doi.org/10.3354/ame01146.

Høgslund, S., N.P. Revsbech, J.G. Kuenen, B.B. Jørgensen, V.A. Gallardo, J. Van De Vossenberg, J. Lund Nielsen, L. Holmkvist, E.T. Arning, and L.P. Nielsen. 2009. Physiology and behaviour of marine Thioploca. *The ISME Journal* 3 (6): 647–657. https://doi.org/10.1038/ismej.2009.17.

Holmes, R.M., J.W. McClelland, D.M. Sigman, B. Fry, and B.J. Peterson. 1998. Measuring $^{15}N–NH_4^+$ in marine, estuarine and fresh waters: an adaptation of the ammonia diffusion method for samples with low ammonium concentrations. *Marine Chemistry* 60 (3-4): 235–243. https://doi.org/10.1016/S0304-4203(97)00099-6.

Ionescu, D., C. Heim, L. Polerecky, V. Thiel, and D. De Beer. 2015. Biotic and abiotic oxidation and reduction of iron at circumneutral pH are inseparable processes under natural conditions. *Geomicrobiology Journal* 32 (3-4): 221–230. https://doi.org/10.1080/01490451.2014.887393.

Jäntti, H., and S. Hietanen. 2012. The effects of hypoxia on sediment nitrogen cycling in the Baltic Sea. *AMBIO* 41 (2): 161–169. https://doi.org/10.1007/s13280-011-0233-6.

Jäntti, H., B.B. Ward, J.W. Dippner, and S. Hietanen. 2018. Nitrification and the ammonia-oxidizing communities in the Central Baltic Sea water column. *Estuarine, Coastal and Shelf Science* 202: 280–289. https://doi.org/10.1016/j.ecss.2018.01.019.

Jenkins, M.C., and W.M. Kemp. 1984. The coupling of nitrification and denitrification in two estuarine sediments. *Limnology and Oceanography* 29 (3): 609–619. https://doi.org/10.4319/lo.1984.29.3.0609.

Joye, S.B., and J.T. Hollibaugh. 1995. Influence of sulfide inhibition of nitrification on nitrogen regeneration in sediments. *Science* 270 (5236): 623–625.

Kalvelage, T., M.M. Jensen, S. Contreras, N.P. Revsbech, P. Lam, M. Günter, J. LaRoche, G. Lavik, and M.M.M. Kuypers. 2011. Oxygen sensitivity of anammox and coupled N-cycle processes in oxygen minimum zones. *PLoS One* 6 (12): e29299. https://doi.org/10.1371/journal.pone.0029299.

Kampschreur, M.J., H. Temmink, R. Kleerebezem, M.S. Jetten, and M.C. van Loosdrecht. 2009. Nitrous oxide emission during wastewater treatment. *Water Research* 43 (17): 4093–4103. https://doi.org/10.1016/j.watres.2009.03.001.

Kemp, W.M., P. Sampou, J. Caffrey, M. Mayer, K. Henriksen, and W.R. Boynton. 1990. Ammonium recycling versus denitrification in Chesapeake Bay sediments. *Limnology and Oceanography* 35 (7): 1545–1563. https://doi.org/10.4319/lo.1990.35.7.1545.

Kessler, A.J., K.L. Roberts, A. Bissett, and P.L. Cook. 2018. Biogeochemical controls on the relative importance of denitrification and dissimilatory nitrate reduction to ammonium in estuaries. *Global Biogeochem Cycles* 32 (7): 1045–1057. https://doi.org/10.1029/2018GB005908.

Kessler, A.J., M. Wawryk, U. Marzocchi, K.L. Roberts, W.W. Wong, N. Risgaard-Petersen, F.J.R. Meysman, R.N. Glud, and P.L. Cook. 2019. Cable bacteria promote DNRA through iron sulfide dissolution. *Limnology and Oceanography* 64 (3): 1228–1238. https://doi.org/10.1002/lno.11110.

Klueglein, N., and A. Kappler. 2013. Abiotic oxidation of Fe (II) by reactive nitrogen species in cultures of the nitrate-reducing Fe (II) oxidizer A cidovorax sp. BoFeN1–questioning the existence of enzymatic Fe (II) oxidation. *Geobiology* 11 (2): 180–190. https://doi.org/10.1111/gbi.12019.

Kraft, B., H.E. Tegetmeyer, R. Sharma, M.G. Klotz, T.G. Ferdelman, R.L. Hettich, J.S. Geelhoed, and M. Strous. 2014. The environmental controls that govern the end product of bacterial nitrate respiration. *Science* 345 (6197): 676–679. https://doi.org/10.1126/science.1254070.

Laanbroek, H.J., and S. Gerards. 1993. Competition for limiting amounts of oxygen between Nitrosomonas europaea and Nitrobacter winogradskyi grown in mixed continuous cultures. *Archives of Microbiology* 159 (5): 453–459.

Lalonde, K., A. Mucci, A. Ouellet, and Y. Gélinas. 2012. Preservation of organic matter in sediments promoted by iron. *Nature* 483 (7388): 198–200. https://doi.org/10.1038/nature10855.

Luettich, R.A. Jr., J.E. McNinch, H.W. Paerl, C.H. Peterson, J.T. Wells, M.J. Alperin, C. S. Martens, and J.L. Pinckney. 2000. Neuse River Estuary modeling and monitoring project stage 1: hydrography and circulation, water column nutrients and productivity, sedimentary processes and benthic-pelagic coupling. Report UNC-WRRI-2000-325B, Water Resources Research Institute of the University of North Carolina, Raleigh, NC, 172p.

McCarthy, M.J., K.S. McNeal, J.W. Morse, and W.S. Gardner. 2008. Bottom-water hypoxia effects on sediment–water interface nitrogen transformations in a seasonally hypoxic, shallow bay (Corpus Christi Bay, TX, USA). *Estuaries and Coasts* 31: 521–531. https://doi.org/10.1007/s12237-008-9041-z.

Master, Y., U. Shavit, and A. Shaviv. 2005. Modified isotope pairing technique to study N transformations in polluted aquatic systems: Theory. *Environmental Science & Technology* 39 (6): 1749–1756. https://doi.org/10.1021/es049086c.

Melton, E.D., E.D. Swanner, S. Behrens, C. Schmidt, and A. Kappler. 2014. The interplay of microbially mediated and abiotic reactions in the biogeochemical Fe cycle. *Nature Reviews Microbiology* 12 (10): 797–3303. https://doi.org/10.1111/1462-2920.12566.

Middelburg, J.J., and L.A. Levin. 2009. Coastal hypoxia and sediment biogeochemistry. *Biogeosciences* 6 (7): 1273–1293. https://doi.org/10.5194/bg-6-1273-2009.

Miranda, K.M., M.G. Espey, and D.A. Wink. 2001. A rapid, simple spectrophotometric method for simultaneous detection of nitrate and nitrite. *Nitric Oxide* 5 (1): 62–71. https://doi.org/10.1006/niox.2000.0319.

Moraghan, J.T., and R.J. Buresh. 1977. Chemical reduction of nitrite and nitrous oxide by ferrous iron 1. *Journal of Environmental Quality* 41 (1): 47–50. https://doi.org/10.2136/sssaj1977.03615995004100010017x.

Murphy, A.E., A.N. Bulseco, R. Ackerman, J.H. Vineis, and J.L. Bowen. 2020. Sulphide addition favours respiratory ammonification

(DNRA) over complete denitrification and alters the active microbial community in salt marsh sediments. *Environmental Microbiology* (in press) 22 (6): 2124–2139. https://doi.org/10.1111/1462-2920.14969.

Murray, R.H., D.V. Erler, and B.D. Eyre. 2015. Nitrous oxide fluxes in estuarine environments: response to global change. *Glob Change Biol* 21 (9): 32193245–32193245. https://doi.org/10.1111/gcb.12923.

Nielsen, L.P. 1992. Denitrification in sediment determined from nitrogen isotope pairing. *FEMS Microbiology Letters* 86 (4): 357–361. https://doi.org/10.1111/j.1574-6941.1992.tb01771.x.

Paerl, H.W., J.L. Pinckney, J.M. Fear, and B.L. Peierls. 1998. Ecosystem responses to internal and watershed organic matter loading: consequences for hypoxia in the eutrophying Neuse River Estuary, North Carolina, USA. *Marine Ecology Progress Series* 166: 17–25. https://doi.org/10.3354/meps166017.

Paerl, H.W., and M.F. Piehler. 2008. Nitrogen and marine eutrophication. In *Nitrogen in the marine environment*, ed. D.G. Capone, M. Mulholland, and E. Carpenter, vol. 2, 529–567. Orlando: Academic Press.

Paerl, H.W., K.L. Rossignol, S.N. Hall, B.L. Peierls, and M.S. Wetz. 2010. Phytoplankton community indicators of short-and long-term ecological change in the anthropogenically and climatically impacted Neuse River Estuary, North Carolina, USA. *Estuaries and Coasts* 33 (2): 485–497. https://doi.org/10.1007/s12237-009-9137-0.

Picardal, F. 2012. Abiotic and microbial interactions during anaerobic transformations of Fe (II) and NOx. *Frontiers in Microbiology* 3: 112. https://doi.org/10.3389/fmicb.2012.00112.

Risgaard-Petersen, N., L.P. Nielsen, S. Rysgaard, T. Dalsgaard, and R.L. Meyer. 2003. Application of the isotope pairing technique in sediments where anammox and denitrification coexist. *Limnology and Oceanography: Methods* 1 (1): 63–73. https://doi.org/10.4319/lom.2003.1.63.

Risgaard-Petersen, N., L.P. Nielsen, S. Rysgaard, T. Dalsgaard, and R.L. Meyer. 2004. Erratum: application of the isotope pairing technique in sediments where anammox and denitrification coexist. *Limnology and Oceanography: Methods* 2 (9): 315. https://doi.org/10.4319/lom.2004.2.315.

Robertson, E.K., K.L. Roberts, L.D. Burdorf, P. Cook, B. and Thamdrup. 2016. Dissimilatory nitrate reduction to ammonium coupled to Fe (II) oxidation in sediments of a periodically hypoxic estuary. Limnology and Oceanography 61: 365–381. https://doi.org/10.1002/lno.10220, 1.

Robertson, E.K., and B. Thamdrup. 2017. The fate of nitrogen is linked to iron (II) availability in a freshwater lake sediment. *Geochimica et Cosmochimica Acta* 205: 84–99. https://doi.org/10.1016/j.gca.2017.02.014.

Schutte, C.A., A. Teske, B.J. MacGregor, V. Salman-Carvalho, G. Lavik, P. Hach, and D. de Beer. 2018. Filamentous giant Beggiatoaceae from Guaymas Basin are capable of both denitrification and dissimilatory nitrate reduction to ammonium (DNRA). *Applied and Environmental Microbiology* 84 (15): e02860–e02817. https://doi.org/10.1128/AEM.02860-17.

Seitzinger, S.P. 1988. Denitrification in freshwater and coastal marine ecosystems: ecological and geochemical significance. *Limnology and Oceanography* 33 (4part2): 702–724. https://doi.org/10.4319/lo.1988.33.4part2.0702.

Sharples, J., J.J. Middelburg, K. Fennel, and T.D. Jickells. 2017. What proportion of riverine nutrients reaches the open ocean? *Global Biogeochem Cycles* 31 (1): 39–58. https://doi.org/10.1002/2016GB005483.

Shields, M.R., T.S. Bianchi, Y. Gelinas, M.A. Allison, and R.R. Twilley. 2016. Enhanced terrestrial carbon preservation promoted by reactive iron in deltaic sediments. *Geophysical Research Letters* 43 (3): 1149–1157. https://doi.org/10.1002/2015GL067388.

Sigman, D.M., M.A. Altabet, R. Michener, D.C. McCorkle, B. Fry, and R.M. Holmes. 1997. Natural abundance-level measurement of the nitrogen isotopic composition of oceanic nitrate: an adaptation of the ammonia diffusion method. *Marine Chemistry* 57: 227–242. https://doi.org/10.1016/S0304-4203(97)00009-1.

Straub, K.L., M.- Benz, B. Schink, and F. Widdel. 1996. Anaerobic, nitrate-dependent microbial oxidation of ferrous iron. *Applied and Environmental Microbiology* 62: 1458–1460.

Sørensen, J., J.M. Tiedje, and R.B. Firestone. 1980. Inhibition by sulfide of nitric and nitrous oxide reduction by denitrifying Pseudomonas fluorescens. *Applied and Environmental Microbiology* 39 (1): 105–108.

van den Berg, E.M., J.L. Rombouts, J.G. Kuenen, R. Kleerebezem, and M.C. van Loosdrecht. 2017. Role of nitrite in the competition between denitrification and DNRA in a chemostat enrichment culture. *AMB Express* 7 (1): 91. https://doi.org/10.1186/s13568-017-0398-x.

Weber, K.A., L.A. Achenbach, and J.D. Coates. 2006. Microorganisms pumping iron: anaerobic microbial iron oxidation and reduction. *Nature Rev Microbiol* 4 (10): 752–764. https://doi.org/10.1038/nrmicro1490.